Appl Microbiol Biotechnol (2017) 101:147–158
DOI 10.1007/s00253-016-7747-6

Characterization of a novel cell wall binding domain-containing *Staphylococcus aureus* endolysin LysSA97

Yoonjee Chang[1] · **Sangryeol Ryu**[1,2]

Received: 16 April 2016 / Revised: 5 July 2016 / Accepted: 20 July 2016 / Published online: 6 August 2016

Abstract Endolysin from *Staphylococcus aureus* phage SA97 (LysSA97) was cloned and investigated. LysSA97 specifically lyse the staphylococcal strains and effectively disrupted staphylococcal biofilms. Bioinformatic analysis of LysSA97 revealed a novel putative cell wall binding domain (CBD) as well as two enzymatically active domains (EADs) containing cysteine, histidine-dependent amidohydrolases/peptidases (CHAP, PF05257) and *N*-acetylmuramoyl-L-alanine amidase (Amidase-3, PF01520) domains. Comparison of 98 endolysin genes of *S. aureus* phages deposited in GenBank showed that they can be classified into six groups based on their domain composition. Interestingly, approximately 80.61 % of the staphylococcal endolysins have a src-homology 3 (SH3, PF08460) domain as CBD, but the remaining 19.39 %, including LysSA97, has a putative C-terminal CBD with no homology to the known CBD. The fusion protein containing green fluorescent protein and the putative CBD of LysSA97 showed a specific binding spectrum against staphylococcal cells comparable to SH3 domain (PF08460), suggesting that the C-terminal domain of LysSA97 is a novel CBD of staphylococcal endolysins.

Electronic supplementary material The online version of this article (doi:10.1007/s00253-016-7747-6) contains supplementary material, which is available to authorized users.

✉ Sangryeol Ryu
sangryu@snu.ac.kr

[1] Department of Food and Animal Biotechnology, Department of Agricultural Biotechnology, Research Institute of Agriculture and Life Sciences, Seoul National University, Seoul 151-921, South Korea

[2] Institute of Food Industrialization, Institutes of Green Bio Science & Technology, Seoul National University, Pyeongchang, Gangwon 232-916, South Korea

Keywords Endolysin · Cell wall binding domain · *Staphylococcus aureus* · Antibacterial

Introduction

Staphylococcus aureus is a highly virulent pathogen that can endanger human and animal health. It causes illnesses such as endocarditis, septicemia, purulent inflammation, toxic shock syndrome, and food poisoning (Chang et al. 2013; Fernandes et al. 2012). *S. aureus* produces biofilm which can cause a variety of problems in the medical and agricultural industries (Arciola et al. 1999; Fox et al. 2005; Melchior et al. 2006). Biofilm is a sessile communities of microorganisms, and the bacteria embedded in biofilms are considerably less susceptible to antibiotics than their planktonic counterparts due to the limited access of the antibiotics (Melchior et al. 2006).

Bacteriophage-encoded peptidoglycan hydrolases, synthesized at the end of the phage life cycle, are essentially produced for the release of phage progeny through rapid breakdown of the infected bacterial peptidoglycan (Gu et al. 2011b; Schmelcher et al. 2015). They have been widely proposed as a potent environmentally friendly substitute for antibiotics (Loeffler et al. 2001; Loessner 2005). Resistance to endolysins is rarer than antibiotics because endolysins have evolved to target unique and essential molecules in the cell wall to avoid becoming trapped inside the host after a phage infection (Fischetti 2008; Schmelcher et al. 2015). It is commonly believed that repeated injection of the endolysin would induce an immune response in the animal. However, the possibility of neutralization of endolysin activity due to immune response was challenged recently by Yang et al. (2014b), who reported that the repeated administration of the endolysin showed no obvious neutralization effect on the lytic activity of the endolysin.

In general, endolysins originating from phages infecting Gram-positives have a modular structure, which contains an enzymatically active domain (EAD) responsible for hydrolysis of peptidoglycans and a cell wall binding domain (CBD) that leads the enzyme specifically to the host bacterial peptidoglycan via non-covalent binding (Loessner 2005). However, relatively little is known about binding mechanisms of CBD. CBD118 and CBD500 from Ply118 and Ply500 endolysins of *Listeria* phages are reported to attach to a ligand present at septal regions and poles (Loessner et al. 2002). Eugster et al. (2011) reported that CBDP35, CBD of *Listeria* phage endolysin PlyP35, specifically interacted with the *N*-acetylglucosamine residue at position C4 of the ribitol phosphate in wall teichoic acid polymers of *L. monocytogenes* serovar 1/2 and 3 strains. Most staphylococcal endolysins are reported to have an src-homology 3 (SH3, PF08460) domain as a CBD (Hugo Oliveira 2013). However, bioinformatic analysis of LysSA97 using BLAST (http://blast.ncbi.nlm.nih.gov/Blast.cgi; Altschul et al. 1997), InterProScan 5 (http://www.ebi.ac.uk/interpro; Jones et al. 2014), and Pfam 28.0 (http://pfam.xfam.org; Finn et al. 2014) revealed two EADs containing cysteine, histidine-dependent amido hydrolases/peptidases (CHAP, PF05257), and *N*-acetyl muramoyl-L-alanine amidase (Amidase-3, PF01520) along with a C-terminal domain not homologous to any known CBDs. Here, we analyzed 98 staphylococcal endolysins reported in GenBank and found that 79 staphylococcal endolysins possess SH3 domain as a CBD. Seven staphylococcal endolysins, including LysSA97, have a novel putative CBD at their C-terminal. The function of this CBD as a specific binder to *Staphylococcus* was also confirmed in this study.

Materials and methods

Bacterial strains, media, and growth conditions

The bacterial strains used in this study are summarized in Table 2. All of these strains were grown in tryptic soy broth (TSB) medium (Difco, Detroit, MI) at 37 °C with shaking, and tryptic soy agar (Difco) containing 1.5 % (*w*/*v*) agar was used for bacterial counting. *Escherichia coli* DH5α and BL21 (DE3) were used in recombinant DNA work for constructing strains containing endolysin gene and were grown in Luria-Bertani (LB) broth (Difco, Detroit, MI) at 37 °C.

Cloning, overexpression, and purification of LysSA97 and LysSA97_CBD

The endolysin gene (SA97_*036*) was analyzed from the SA97 phage genome (GenBank accession number KJ716334; Chang et al. 2015) and was amplified by polymerase chain reaction (PCR) with the primers lysSA97F and lysSA97R in Table 1. The PCR condition consisted of initial denaturation step at 100 °C for 10 min, followed by 30 cycles of denaturation step at 95 °C for 30 s, annealing at 55 °C for 30 s, and elongation at 72 °C for 1 min 20 s, and final extension step at 72 °C for 7 min. The PCR product was cloned into a pET28a vector (Novagen, Madison, WI), which had N-terminal hexahistidine (His)-tag sequences. Next, it was transformed into *E. coli* BL21 (DE3). The T7 promoter was induced with 0.5 mM isopropyl-*β*-thiogalactopyranoside (IPTG) at OD_{600} 0.8 to express the endolysin LysSA97, followed by incubation at 18 °C for 22 h. The bacteria were suspended in phosphate lysis buffer (20 mM sodium phosphate, 300 mM sodium chloride, pH 7.0) and disrupted by sonication (Branson Ultrasonics, Danbury, CT). The cells were centrifuged at 15,000×*g* for 30 min to obtain supernatant containing soluble protein, which was passed through a Ni-NTA superflow column (Qiagen Gmbh, Germany) to acquire purified protein. After this, we moved the purified protein to storage buffer (20 mM sodium phosphate, 300 mM sodium chloride, pH 7.0, 50 % glycerol) using a PD Miditrap G-25 (GE healthcare, Amersham, Bucks, UK) to store the protein at −20 °C until use.

The green fluorescent protein (GFP) fusion to LysSA97_CBD (LysSA97_CBD-GFP) was then constructed. Putative CBD regions were determined by the domain analysis of LysSA97. CHAP was located at the N-terminus, amidase-3 (*N*-acetylmuramoyl-L-alanine amidase) at the middle region, and no homolog was at the C-terminus. Therefore, we predicted that the putative CBD would be next to amidase-3 (*N*-acetylmuramoyl-L-alanine amidase), in the 368 to 470 region of LysSA97. For strain construction, LysSA97_CBD was amplified by PCR with the primers lysSA97_CBD-F and lysSA97_CBD-R in Table 1, and cloned into a pET28a-containing GFP (pET28a-GFP) vector. The T7 promoter was induced with 0.5 mM IPTG at exponential growth to express the LysSA97_CBD-GFP, followed by incubation at 37 °Cfor 3 h. Subsequently, protein purification was conducted as previously described (Gu et al. 2011a).

Turbidity reduction assay

The lytic activities against *S. aureus* RN4220 were assessed by turbidity reduction assay (Gaeng et al. 2000). Bacterial cells were incubated to an early-exponential phase, harvested, and resuspended with reaction buffer (50 mM sodium phosphate, pH 7.0). In the case of Gram-negative bacteria, cells were pre-treated with 50 mM sodium phosphate buffer with 0.1 M EDTA for 5 min at room temperature (RT) and the cells were washed three times, as previously described (Leive 1968). Various amounts (0–200 μg) of the endolysins and the bacterial cell suspensions were mixed thoroughly and incubated at RT, and OD_{600} values were monitored over time.

Table 1 Oligonucleotide primers used for cloning

Primer	Nucleotide sequences [5 → 3][a]	Restriction sites	Reference
lysSA97F	GGAGATGATACATATGCCGT CGGTTA	*Nde*I	This study
lysSA97R	AATAACCTACCTCGAGTCTTTTTATA	*Xho*I	This study
lysSA97_CBD-F	GATGCGCCAGGATCCAAGCCAAGC	*Bam*HI	This study
lysSA97_CBD-R	AATAACCTACCTCGAGTCTTTTTATA	*Xho*I	This study

[a] Restriction sites are underlined

To test the pH stability, 50 μg of LysSA97 was added to the *S. aureus* RN4220 cell suspension with various buffers: 0.1 % trifluoroacetic acid (pH 2.0), 50 mM sodium acetate (pH 4.0), 50 mM 2-(*N*-morpholino) ethanesulfonic acid (pH 6.0), 50 mM bis-tris (pH 7.0), 50 mM tris–HCl (pH 8.0), and 50 mM *N*-cyclohexyl-3-aminopropanesulfonic acid (pH 10.0). To assess the effect of temperature on LysSA97 enzymatic activity, different temperatures (4–65 °C) were set and the endolysin was incubated in each group for 30 min. Next, the turbidity reduction assay was applied to *S. aureus* RN4220. The influence of NaCl on lysis activity was evaluated under various conditions with several different NaCl concentrations (0–300 mM) at RT (Son et al. 2012).

Plate lysis assay

Plate lysis assays were performed as previously described (Becker et al. 2009). In brief, purified protein was diluted in sterile phosphate-buffered saline (PBS). Twenty microliters containing 50 μg of the protein was spotted onto a freshly spread lawn of mid-log phase of bacterial cells that had air-dried for 10 min on TSA plates. Spotted plates were air-dried in a laminar flow hood (15 min) and incubated overnight at 37 °C. Cleared spots were scored within 20 h of plating. Lysis with clear zone was considered as a positive result.

Biofilm reduction assay

A biofilm disruption assay was performed as previously described with some modifications (Wu et al. 2003). *S. aureus* Newman incubated in BHI medium supplemented with 0.25 % D-(+)-glucose (Sigma) was prepared and was sub-cultured to the same media in a 96-well polystyrene microplate. Glucose was supplemented to the medium as it can induce the biofilm formation by inducing *ica* gene (Jin et al. 2005) and most of the staphylococci adhered to the plates in glucose-rich medium than in glucose-poor medium (Moreira et al. 2013). After incubating the microplate for 24 h at 37 °C, all wells were washed with PBS. Once the biofilm was formed, the experimental group wells were filled with LysSA97 (50 μg), whereas PBS was added to the negative control. After the incubation for 2 h at 37 °C, each well was washed once with PBS and stained with 0.1 % crystal violet. Additional washing with PBS, followed by solubilizing with 33 % acetic acid, was done. The absorbance of the obtained solution was measured at 570 nm and the sessile biomass was presented as the OD_{570} value (Salazar et al. 2013; Simoes et al. 2007; Son et al. 2010).

To prepare samples for scanning electron microscopy (SEM), the procedures of the biofilm assay on glass cover slips in a six-well culture plate (Corning, NewYork, NY, USA) instead of a 96-well microplate as described above. The microscopic sample was prepared following a previously reported method (Wu et al. 2003). A field-emission scanning electron microscope (SUPRA 55VP, Carl Zeiss, Germany) was used to observe the biofilm formation.

Bioinformatics analysis of staphylococcal endolysins

The LysSA97 endolysin gene (SA97_*036*) was identified in the SA97 phage genome in a previous study (Chang et al. 2015). Its protein domain composition was analyzed using the BLAST (http://blast.ncbi.nlm.nih.gov/Blast.cgi; Altschul et al. 1997), InterProScan 5 (http://www.ebi.ac.uk/interpro; Jones et al. 2014), and Pfam 28.0 (http://pfam.xfam.org; Finn et al. 2014) programs. The nucleotide sequences of 98 *S. aureus* phages on NCBI were analyzed and the putative endolysin genes were identified. The bioinformatics analysis of the domain compositions of staphylococcal endolysins revealed six distinct groups of endolysin.

To determine the phylogenetic position of the LysSA97 endolysin and its CBD, respectively, phylogenetic trees were constructed based on the alignment of the amino acid sequences from the full-length endolysins and their CBDs from 98 staphylococcal endolysins. The amino acid sequences used for phylogenetic trees are available online in the NCBI nucleotide databases (http://www.ncbi.nlm.nih.gov/nuccore). Alignments of amino acid sequences were aligned using the Clustal ×2 program (Larkin et al.

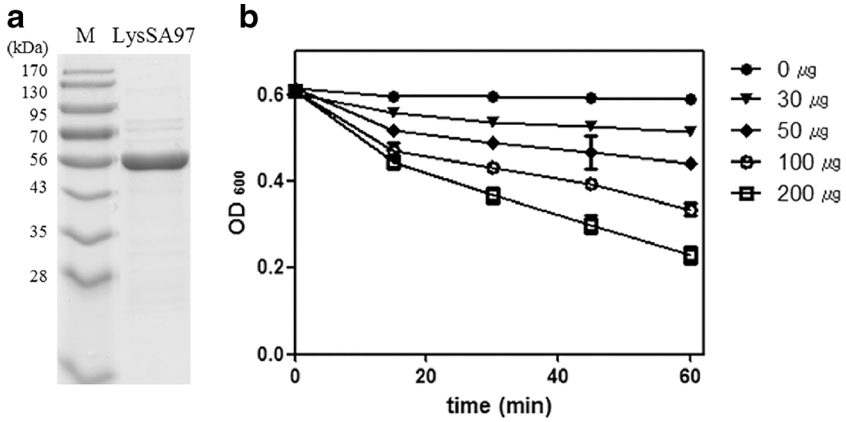

Fig. 1 Purification and lytic activities of LysSA97. **a** Purified LysSA97 was loaded on an SDS-PAGE gel. *Lane M*, standard molecular weight marker; *LysSA97*, purified LysSA97 fraction. **b** Lysis of *S. aureus* RN4220 in the presence of recombinant LysSA97. *Black circle* negative control (no enzyme added), *inverted black triangle* 30 μg enzyme added, *black diamond* 50 μg enzyme added, *circle* 100 μg enzyme added, *square* 200 μg enzyme added. The data shown are the mean values from three independent measurements and the *error bars* represent the standard deviations

2007). Phylogenetic trees based on the alignments of protein amino acid sequences were constructed and obtained bootstrap neighbor-joining trees (B = 1,000 of bootstrap replications) using the MEGA5 program (Kumar et al. 2008).

Amidase assay

N-acetylmuramyl-L-alanine amidase activity was measured by quantification of acetaldehyde in the peptidoglycan after the endolysin reaction. *S. aureus* peptidoglycan was prepared as previously described (Fein and Rogers 1976; Kuroda and Sekiguchi 1990). The bacterial cell was disrupted by sonication and centrifuged at low speed (1,400×*g*, 10 min) to remove the unbroken cells. Only the supernatant was recentrifuged at high speed (27,000×*g*, 5 min) to obtain the crude cell wall pellet, suspended in 4 % SDS solution, and boiled for 10 min. It was washed three times after cooling and resuspended in endolysin reaction buffer (50 mM sodium phosphate, pH 7.0). Negative control groups were composed of peptidoglycan solution only or reaction buffer containing LysSA97 (50 μg) each, and the group with the reaction buffer was set for the reference. For the experimental group, 200 μg of peptidoglycan solution containing 50 μg of lysSA97 was prepared, and all of these groups were incubated at RT for 1 h. To stop the reaction, 1.0 M NaOH was mixed into each reaction. After 30 min incubation at 38 °C, 0.5 M H_2SO_4 and concentrated H_2SO_4 (5 mL) were added to each set. The stoppered tubes were placed in boiling water for 5 min. After cooling on ice, 4 % $CuSO_4 \cdot 5H_2O$ and 1.5 % ρ-hydroxydiphenyl solution were added and incubated for 30 min at 30 °C. Finally, the OD_{560} was measured (Hadzija 1974; Hazenberg and de Visser 1992) with the supernatants. Briefly, muramic acid, which was used as the standard, was degraded to lactic acid by *N*-acetylmuramyl-L-alanine amidases, the lactic acid was then degraded to acetaldehyde, and finally, the color was changed by the reaction with ρ-hydroxydiphenyl (Park et al. 2012).

Binding assessment of GFP fusion protein to the bacterial cell

One milliliter of early-exponential-phase cell cultures were collected and resuspended in 100 μl PBS. The cells were incubated with 0.8 μM of GFP fused LysSA97_CBD protein for 5 min at RT. After incubation, the cells were collected by centrifugation at 16,000×*g* for 1 min, washed, and resuspended in PBS. GFP alone was used as a negative control to test if GFP has any binding affinity for bacterial cell surfaces. A super-resolution confocal microscope (Leica, SP8 X STED, Germany) was used to detect the fluorescence of the treated cells to determine the binding specificity of LysSA97_CBD (Gu et al. 2011a).

Statistical analysis

Statistical analysis was conducted using the GraphPad Prism program (version 5.01). All results were analyzed by Student's unpaired t test. The data are presented as means and standard deviations. A P value of <0.05 was considered statistically significant.

Nucleotide sequence accession number

The complete genome sequence of *S. aureus* phage SA97 has been deposited in GenBank under accession number KJ716334.

Results

Overexpression and lytic activities of LysSA97 endolysin

The endolysin gene was identified from the genome sequence of phage SA97 (Chang et al. 2015), cloned, and overexpressed in *E. coli*. LysSA97 was purified to near homogeneity (Fig. 1a). This preparation showed concentration-dependent cell lysis activity (Fig. 1b). To examine the susceptibility of various strains against LysSA97, plate lysis assay was performed. LysSA97 could lyse the bacterial cells confined to staphylococcal species (Table 2).

Lytic activity analysis at different pH values demonstrated that LysSA97 was relatively stable under pH ranges between 6.0 and 8.0, with the highest activity at pH 7.0 (Fig. 2a). LysSA97 was highly active under the temperature ranges between 25 and 37 °C (Fig. 2b). Its activity was relatively stable under wide ranges of NaCl concentrations up to 300 mM, with the maximum activity level at 0 mM NaCl conditions (Fig. 2c).

Table 2 The antimicrobial spectrum of LysSA97, cell wall binding spectrum of LysSA97_CBD, and SH3 domain (PF08460)

Bacterial strain	Lysis zone formation of LysSA97	Binding activity of LysSA97_CBD	Binding activity of SH3 domain (PF08460)[b]	Reference or source
***Staphylococcus* strains**				
Staphylococcus aureus RN4220	+	+	+	Park et al. (2010)
Staphylococcus aureus Newman	+	+	+	Baba et al. (2008)
Staphylococcus aureus KCTC 1916	+	+	+	KCTC
Staphylococcus aureus ATCC 6538	+	+	+	ATCC
Staphylococcus aureus ATCC 23235	+	+	+	ATCC
Staphylococcus aureus ATCC 25923	+	+	+	ATCC
Staphylococcus aureus ATCC 29213	+	+	+	ATCC
Staphylococcus aureus ATCC 33593	+	+	+	ATCC
Staphylococcus aureus ATCC 33586	+	+	+	ATCC
Methicillin resistant *S. aureus* CCARM 3089	+	+	+	CCARM
Methicillin resistant *S. aureus* CCARM 3090	+	+	+	CCARM
Methicillin resistant *S. aureus* CCARM 3793	+	+	+	CCARM
Staphylococcus aureus ATCC 12600	−	+	+	ATCC
Staphylococcus aureus ATCC 13301	−	+	+	ATCC
Staphylococcus xylosus, ATCC 29971	+	+	+	ATCC
Staphylococcus hominis, ATCC 37844	+	+	+	ATCC
Staphylococcus capitis, ATCC 35661	+	+	+	ATCC
Staphylococcus saprophyticus, ATCC 15305	+	+	+	ATCC
Staphylococcus haemolyticus, ATCC 29970	+	+	+	ATCC
Staphylococcus intermedius, ATCC 29663	+	+	+	ATCC
Staphylococcus epidermidis ATCC 35983	−	+	+	ATCC
Staphylococcus warneri ATCC 10209	+	+	−	ATCC
Other Gram-positive bacteria				
Enterococcus faecalis ATCC 29212	−	−	−	ATCC
Bacillus cereus ATCC 14579	−	−	−	ATCC
Bacillus subtilis ATCC 23857	−	−	−	ATCC
Listeria monocytogenes ATCC 19114	−	−	−	ATCC
Gram-negative bacteria				
Salmonella enterica serovar Typhimurium SL1344	-[a]	-[a]	-[a]	ATCC
E. coli O157:H7 ATCC 35150	-[a]	-[a]	-[a]	ATCC
Cronobacter sakazakii ATCC 29544	-[a]	-[a]	-[a]	ATCC
Pseudomonas aeruginosa ATCC 27853	-[a]	-[a]	-[a]	ATCC

[a] Gram-negative bacteria were treated with EDTA

[b] Binding activities were examined by LysSA12_CBD involved in type III (GenBank accession no. NC_021801.1)

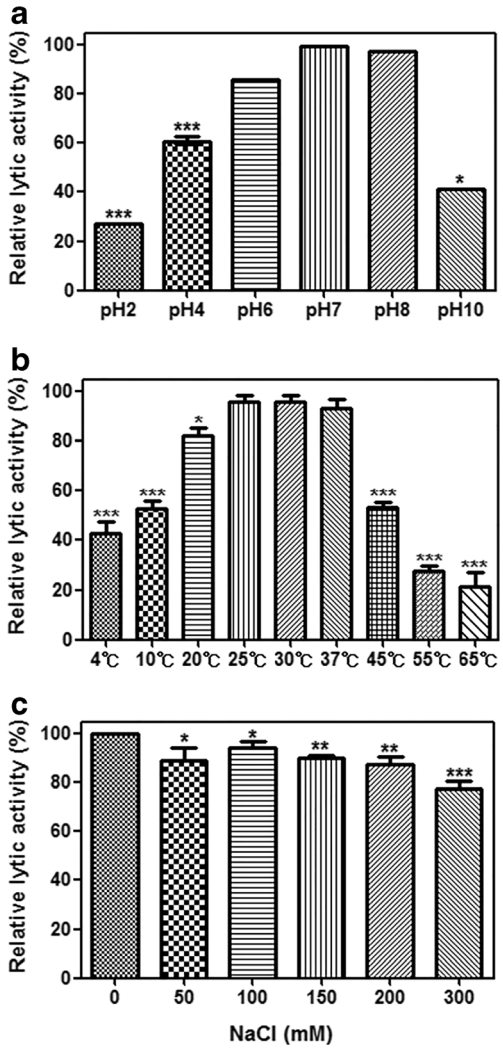

Fig. 2 Effect of pH, temperature, and NaCl on the lytic activities of LysSA97. The effect of pH (**a**), temperature (**b**), and NaCl concentration (**c**) on the lytic activities of LysSA97 against *S. aureus* RN4220 cells are shown. Each *column* represents the mean of triplicate experiments and *error bars* indicate the standard deviation. The *asterisks* indicate significant differences (***$P < 0.001$, **$P < 0.01$, *$P < 0.05$)

Biofilm reduction activity of LysSA97

The biofilm matrix disruption by LysSA97 endolysin was verified by visual comparison in crystal violet-staining and SEM. Although the biofilm removal extent was sufficient to be determined by visual examination, it was further confirmed by quantification of crystal violet staining. As shown in Fig. 3a, the blue-stained color was significantly reduced in the LysSA97-treated group compared with the PBS-treated control group. Approximately 90 % of the biofilm was reduced in the LysSA97 endolysin-treated group compared with the control. Most biofilms formed after 24 h incubation of *S. aureus* Newman cells were removed and a few cells remained on the glass surface were deformed after treatment with 50 μg of LysSA97 for 2 h (Fig. 3b).

Functional domains of LysSA97

LysSA97 is composed of 470 amino acids (55.4 kDa). BLAST (Altschul et al. 1997), InterProScan 5 (Jones et al. 2014), and Pfam 28.0 (Finn et al. 2014) analysis suggested that LysSA97 is a putative *N*-acetylmuramoyl-L-alanine amidase consisting of an N-terminal CHAP domain (PF05257; *E* value, 3.9e-12) and a middle amidase-3 domain (*N*-acetylmuramoyl-L-alanine amidase, PF01520; *E* value, 1.1e-23), known as the enzymatic domains that cleave the amide bond between the *N*-acetylmuramoyl and L-alanine residues in bacterial cell walls (Hugo Oliveira et al. 2013; Szweda et al. 2012). Amino acid sequence alignment revealed that LysSA97 presents 100 % overall identity with a CHAP domain containing protein of *S. aureus* JH9.

To confirm the predicted amidase activity of LysSA97, the quantity of free muramic acid on the *N*-acetylmuramic acid residue was analyzed (Hadzija 1974). As shown in Fig. 4, the amount of muramic acid in the peptidoglycan significantly increased within 1 h after the endolysin reaction. When LysSA97 was applied to the *S. aureus* peptidoglycan, free muramic acid production was 4.83 times more than in the control groups that means LysSA97 cleaves the lactate link between the *N*-acetylmuramic acid and L-alanine of the peptide side chain. Therefore, LysSA97 was demonstrated to have amidase activity.

However, the BLAST, InterProScan 5, and Pfam 28.0 analysis of LysSA97 did not reveal a CBD homologous to the known CBD even though most reported staphylococcal endolysins are known to have SH3 domain (PF08460) as a CBD (Becker et al. 2009; Hugo Oliveira et al. 2013) (Table 3). This suggests that LysSA97 may have a novel CBD because it has a C-terminal domain large enough to function as a CBD in addition to the EAD.

Grouping of staphylococcal endolysins

EADs and CBDs of 98 known *S. aureus* endolysins (April 2015) were predicted and compared to evaluate the possibility of the C-terminal domain of LysSA97 as a novel CBD. Staphylococcal endolysins have several distinct domain compositions; most have two EADs (CHAP and amidase-2 (*N*-acetylmuramoyl-L-alanine amidase) or amidase-3 (*N*-acetylmuramoyl-L-alanine amidase)), and some have

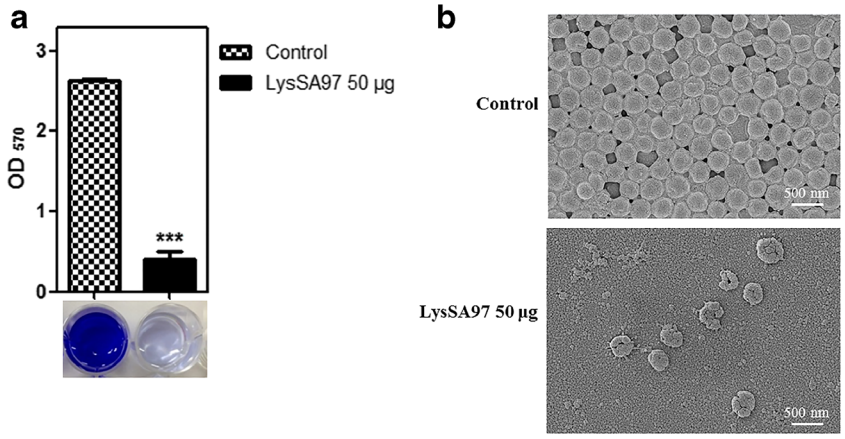

Fig. 3 Examination of the *S. aureus* biofilm disruption abilities by LysSA97 treatment. **a** Biofilms after crystal violet-staining were shown. *Left well* negative control treated with PBS, *right well* the experimental group applied with purified LysSA97 (50 μg). The *dark staining* indicates the existence of a biofilm that is maintained after treatment for biofilm disruption and *light staining* indicates the successful removal of biofilm. The biomass amount was presented as the OD_{570} value. Each *column* represents the mean standard deviations of triplicate assays. The *asterisks* indicate significant differences (***$P < 0.001$). **b** Scanning electron microscope analysis of the degradation efficacy of LysSA97 against *S. aureus* Newman biofilms. *Control* indicates the sample treated with PBS; *LysSA97 50 μg* indicates the sample treated with 50 μg of LysSA97. Magnification ×10,000 and *scale bar* indicates 500 nm

CHAP as a single EAD; however, not all staphylococcal endolysins have SH3 domain as a CBD, contrary to previous reports (Oliveira et al. 2013). All of the endolysins, except the 2638A endolysin, have CHAP as EAD in the N-terminal. Therefore, the endolysins can be divided into six groups based on their domain compositions. Group I contains endolysins containing CHAP as a catalytic domain and a putative CBD not homologous to any known CBD and group II contains those with CHAP and SH3 domains. Endolysins with CHAP/amidase-2 (*N*-acetylmuramoyl-L-alanine amidase)/SH3 domains are in group III and those with CHAP/amidase-3 (*N*-acetylmuramoyl-L-alanine amidase)/SH3 domains are in group IV. Group V contains endolysins with both CHAP and amidase-3 (*N*-acetylmuramoyl-L-alanine amidase) but with another putative CBD not homologous to any known CBD, and group VI contains endolysins with peptidase_M23 (PF01551)/amidase-2 (*N*-acetylmuramoyl-L-alanine amidase)/SH3 domains.

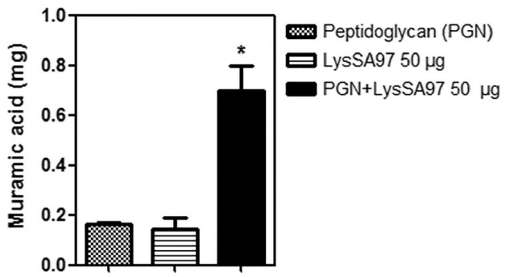

Fig. 4 *N*-acetylmuramyl-L-alanine amidase activities of LysSA97. Peptidoglycan (PGN) extracted from *S. aureus* RN4220 was incubated with or without 50 μg of purified LysSA97. The level of released muramic acid was measured after 1 h endolysin incubation. *Peptidoglycan (PGN)* peptidoglycan only, *LysSA97 50 μg* LysSA97 only, *PGN + LysSA97 50 μg* 50 μg LysSA97 was added to the PGN. Each *column* represents the mean standard deviations of triplicate assays. The *asterisk* indicates significant differences (*$P < 0.05$)

According to the InterProscan 5 results, firstly we divided staphylococcal endolysin CBDs into two groups, SH3 domain and unknown. Interestingly, 19 out of 98 endolysins contained putative CBDs with no homology to the known CBD, SH3 domain. Further, we divided the unknown group again into two groups, type I_CBD and type V_CBD, according to the amino acid sequence alignment results through BLAST align analysis. LysSA97, together with six other endolysins in group V, contains a putative CBD with more than 97 % similarity, and endolysins in group I contain other putative CBDs not homologous to those in group V endolysins, suggesting that at least two more types of CBDs exist in staphylococcal endolysins in addition to the well-known SH3 domain (Table 3).

To compare the genomes of the staphylococcal full-length endolysins and their CBDs, phylogenetic analysis was performed based on their amino acid sequences (Fig. S1 and **5**, respectively). The results were comparable to the grouping analysis by domain compositions (Table 3). Especially, phylogenetic analysis of the CBD sequences revealed that

Table 3 Staphylococcal endolysins grouping based on the domain compositions

Group	Domain composition	Phages containing the same group endolysin
Type I	EAD (CHAP) and CBD (no homology 1)	42E, 187, SAP-26, SAP090B, phi13, phiBU01, phiPV83, phiNM3, phiN315, tp310–3, P954, and JS01
Type II	EAD (CHAP) and CBD (SH3 domain)	44HJD, 66, P68, SAP-2, S13, S24-1, GRCS, vB_SauM_Remus, vB_SauM_Romulus, SA5, and ISP
Type III	EAD (CHAP, amidase-2 (*N*-acetylmuramoyl-L-alanine amidase)) and CBD (SH3 domain)	11, 29, 37, 52A, 55, 69, 80, 85, 88, 92, 676Z, A3R, A5W, DW2, JD007, Fi200W, MSA6, ×2, EW, P4W, GH15, K, MCE-2014, Sb-1, SP5, SP6, SA12, SA13, Staph1N, S25-3, S25-4, phiMR11, phiMR25, phiNM2, phiSauS-IPLA88, phiSA012, phiIPLA-C1C, phiIPLA-RODI, and 812
Type IV	EAD (CHAP, amidase-3 (*N*-acetylmuramoyl-L-alanine amidase)) and CBD (SH3 domain)	3 A, 53, 96, 77, 80alpha, ROSA, TEM123, TEM126, tp310–1, tp310–2, SMSAP5, StauST398–4, LH1, PVL, phiNM, phi12, phiSauS-IPLA35, phiPVL108, phi2958PVL, phiPVL-CN125, phiNM1, phiNM4, phiSa119, phiSLT, phi5967PVL, phi7247PVL, phi7401PVL, and YMC/09/04/R1988
Type V	EAD (CHAP, amidase-3 (*N*-acetylmuramoyl-L-alanine amidase)) and CBD (no homology 2)	phiETA, phiETA2, phiETA3, 71, StauST398–1, StauST398–5, and SA97
Type VI	EAD (peptidase_M23, amidase-2 (*N*-acetylmuramoyl-L-alanine amidase)) and CBD (SH3 domain)	2638A

LysSA97_CBD was involved in type V and totally different from another non-SH3 domain CBD in type I (Fig. 5). Two endolysins from the phage SA5 (GenBank accession no. JX875065.1) and ISP (GenBank accession no. FR852584.1) were classified into type II according to the domain compositions; however, both of their full-length and CBD genome sequences were revealed to be more similar to type III (Fig. S1 and 5). The results seemed to be occurred as amidase-2 (*N*-acetylmuramoyl-L-alanine amidase) domain was missing in those two endolysins because of some gene mutation. In the case of the phage 2638A endolysin in type VI, its CBD (SH3 domain) was similar to the CBD in type III, even though the genome sequences of the full-length endolysin was totally different from others.

Confirmation of the C-terminal domain of LysSA97 as a novel CBD

To confirm the bacterial binding activity of a putative CBD of LysSA97, a fusion protein containing the predicted CBD region (amino acid residues 368–470) and GFP was cloned into a pET28a vector and purified (Fig. 6a). Purified GFP or GFP-LysSA97_CBD was added to *S. aureus* cells and binding was viewed by fluorescence microscopy. GFP alone did not show any binding affinity to the bacterial cells as a control in Fig. 6b. The LysSA97_CBD binding spectrum covered entire staphylococcal strains tested including 14 *S. aureus* and 8 of other staphylococcal strains known to be harmful to human (Cone et al. 2005; Cuong Vuong 2002; Daniel et al. 2014; Hovelius and Mardh 1984; Theodoros Kelesidis 2010; Voineagu et al. 2012; Won et al. 2002) (Table 2). However, no binding of fusion protein to any other bacteria tested was observed under the same conditions (Table 2).

Discussion

Endolysins are promising biocontrol or therapeutic agents as they show specific action spectrum and low incidence of resistance (Obeso et al. 2008; Oliveira et al. 2012). In this study, the novel endolysin LysSA97 containing unprecedented CBD was characterized. LysSA97 could lyse the bacterial cells confined to staphylococcal species (Table 2), suggesting that it may hydrolyze analogous peptidoglycan structure with the amide linkage between *N*-acetylmuramic acid and L-alanine, commonly found in various staphylococcal strains (Schleifer and Kandler 1972). LysSA97 killed a large number of staphylococcal strains in a wide range of pH, temperature, and NaCl concentrations (Fig. 2) that could be a good biocontrol agent.

LysSA97 endolysin could remove staphylococcal biofilms effectively as observed by SEM (Fig. 3). It is likely that LysSA97 endolysin lyses individual staphylococcal cells embedded in the extracellular matrix of the biofilm, resulting in destabilization of the biofilm and its detachment from the surfaces as suggested by previous studies (Fenton et al. 2013; Shen et al. 2013; Son et al. 2010; Yang et al. 2014a). These results demonstrate that LysSA97 can be used to treat infections such as osteomyelitis, periodontitis, and chronic rhinosinusitis (Archer et al. 2011) caused by biofilm-forming *S. aureus* cells.

Endolysins originating from phages infecting Gram-positives form a modular structure containing EADs and

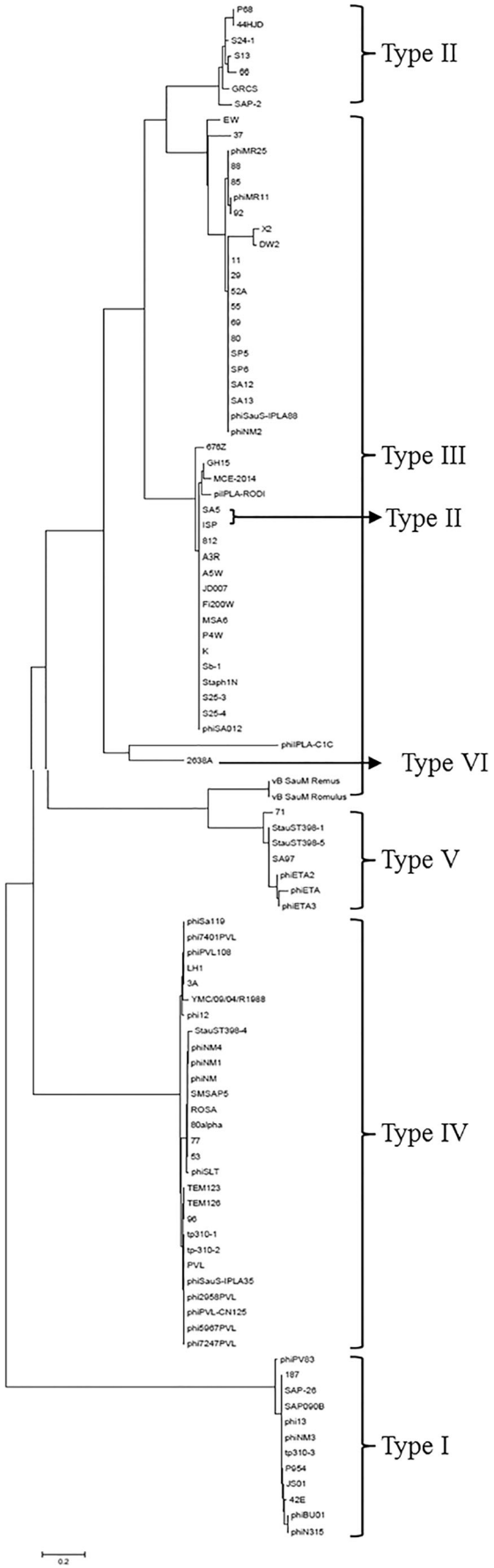

◀ **Fig. 5** Phylogenetic analysis of the CBD sequences of 98 staphylococcal endolysins. The phylogenetic tree was generated with the neighbor-joining method with *P* distance values using the MEGA5 program

CBD and most reported endolysins lysing *S. aureus* were known to have a SH3 domain as a CBD (Becker et al. 2009; Oliveira et al. 2013). However, the BLAST, InterProScan 5, and Pfam 28.0 analysis of LysSA97 did not reveal a CBD homologous to the known CBD, a SH3 domain (Table 3). This suggests that LysSA97 may have an unusual CBD because it has a C-terminal domain large enough to function as a CBD in addition to the EAD. The minimum amino acid residues required for specific binding of LysSA97_CBD were studied. The systematic truncations of LysSA97_CBD were fused to GFP and their bindings were compared; LysSA97_CBD trunc1 containing the amino acid residues from 371 to 470, LysSA97_CBD trunc2 containing the amino acid residues from 386 to 470, LysSA97_CBD trunc3 containing the amino acid residues from 386 to 453, LysSA97_CBD trunc4 containing the amino acid residues from 398 to 453, and LysSA97_CBD trunc5 containing the amino acid residues from 386 to 435 of the LysSA97 were made and their bindings to *S. aureus* were compared. Binding assay revealed that the minimum amino acid residues required for specific binding to *S. aureus* RN4220 was residues from 386 to 453 (Fig. S2).

The green fluorescent protein and the putative CBD of LysSA97 fusion protein showed a specific binding spectrum against staphylococcal cells comparable to SH3 domain except *Staphylococcus warneri* ATCC 10209 (Table 2**,** Fig. 6), suggesting that the C-terminal domain of LysSA97 is a novel CBD of staphylococcal endolysins. At least eight different types of peptidoglycan exist in Gram-positive bacteria (Schleifer and Kandler 1972). Other Gram-positive bacteria tested in this study (Table 2) have different cell wall types without glycine-rich interpeptide bridges. *Staphylococcus* have A3α type which possess penta-glycine structure while both *Listeria* (Kamisango et al. 1982) and *Bacillus* have A1γ type (Regulski et al. 2013) and *Enterococcus* have D-Asx cross bridges instead of glycine-rich bridges in peptidoglycan structure (Hendrickx et al. 2013). As LysSA97_CBD is specifically bound to staphylococci, we could predict that it might be attached to distinctive region in staphylococcal cells, such as pentaglycine cross bridge structure which is already known as a binding site of SH3 domain of lysostaphin (Grundling and Schneewind 2006). These results indicate that the LysSA97_CBD is a novel CBD of staphylococcal endolysins which targets specifically to the envelope of staphylococci, representing a potential use of LysSA97_CBD as a bioprobe for detecting staphylococcal cells.

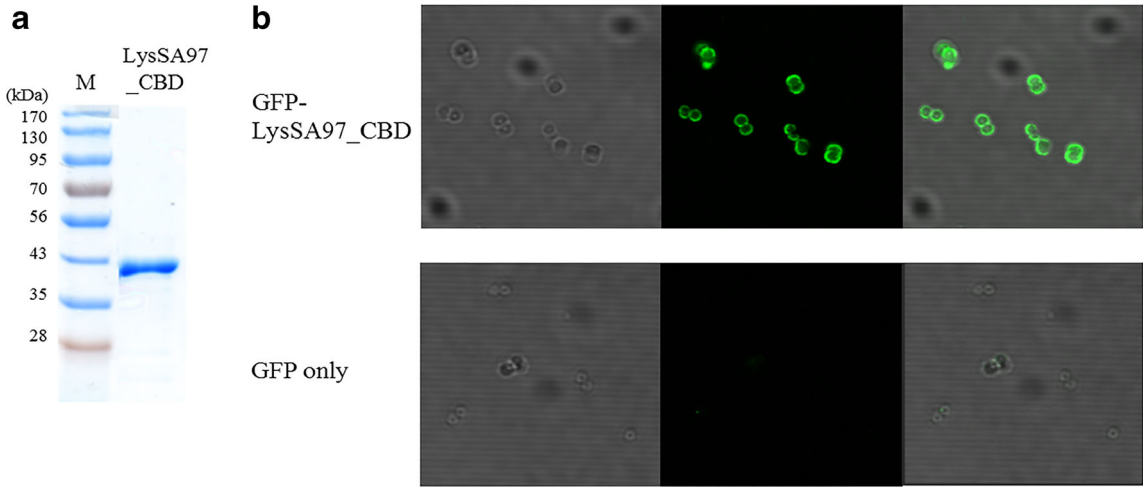

Fig. 6 Purification and binding activity of LysSA97_CBD. **a** Purified LysSA97_CBD was loaded on an SDS-PAGE gel. *Lane M* standard molecular weight marker, *LysSA97_CBD* purified fraction of LysSA97_CBD. **b** *GFP-LysSA97_CBD* LysSA97_CBD directly interacted with *S. aureus* RN4220, *GFP only* GFP alone did not bind to *S. aureus*. Images represent bright field (*left*), fluorescent (*middle*), and merged (*right*) states

Acknowledgments We thank Dr. Bok Luel Lee at Pusan National University for sharing *S. aureus* strains (Newman and RN4220 wild-type strains). This work was supported by Agriculture, Food and Rural Affairs Research Center Support Program, Ministry of Agriculture, Food and Rural Affairs, and the National Research Foundation of Korea (NRF) grant funded by the MSIP (NRF-2014R1A2A1A10051563), Republic of Korea.

Compliance with ethical standards This article does not contain any studies with human participants or animals performed by any of the authors.

Conflict of interest The authors declare that they have no conflict of interest.

References

Altschul SF, Madden TL, Schaffer AA, Zhang J, Zhang Z, Miller W, Lipman DJ (1997) Gapped BLAST and PSI-BLAST: a new generation of protein database search programs. Nucleic Acids Res 25: 3389–3402. doi:10.1093/nar/25.17.3389

Archer NK, Mazaitis MJ, Costerton JW, Leid JG, Powers ME, Shirtliff ME (2011) *Staphylococcus aureus* biofilms properties, regulation and roles in human disease. Virulence 2:445–459. doi:10.4161/viru.2.5.17724

Arciola CR, Montanaro L, Baldassarri L, Borsetti E, Cavedagna D, Donati E (1999) Slime production by staphylococci isolated from prosthesis-associated infections. New Microbiol 22:337–341. doi:10.1007/978-1-4471-3454-1_55

Baba T, Bae T, Schneewind O, Takeuchi F, Hiramatsu K (2008) Genome sequence of *Staphylococcus aureus* strain Newman and comparative analysis of staphylococcal genomes: polymorphism and evolution of two major pathogenicity islands. J Bacteriol 190:300–310. doi:10.1128/JB.01000-07

Becker SC, Foster-Frey J, Stodola AJ, Anacker D, Donovan DM (2009) Differentially conserved staphylococcal SH3b_5 cell wall binding domains confer increased staphylolytic and streptolytic activity to a streptococcal prophage endolysin domain. Gene 443:32–41. doi:10.1016/j.gene.2009.04.023

Chang Y, Lee JH, Shin H, Heu S, Ryu S (2013) Characterization and complete genome sequence analysis of *Staphylococcus aureus* bacteriophage SA12. Virus Genes 47:389–393. doi:10.1007/s11262-013-0938-7

Chang Y, Shin H, Lee JH, Park C, Paik S, Ryu S (2015) Isolation and genome characterization of the virulent *Staphylococcus aureus* bacteriophage SA97. Viruses 7:5225–5242. doi:10.3390/v7102870

Cone LA, Sontz EM, Wilson JW, Mitruka SN (2005) *Staphylococcus capitis* endocarditis due to a transvenous endocardial pacemaker infection: case report and review of *Staphylococcus capitis* endocarditis. Int J Infect Dis 9:335–339. doi:10.1016/j.ijid.2004.08.004

Cuong Vuong MO (2002) *Staphylococcus epidermidis* infections. Microbes Infec 4:481–489. doi:10.1016/S1286-4579(02)01563-0

Daniel B, Saleem M, Naseer G, Fida A (2014) Significance of *Staphylococcus haemolyticus* in hospital acquired infections. J Pioneer Med Sci 4:119–125

Eugster MR, Haug MC, Huwiler SG, Loessner MJ (2011) The cell wall binding domain of *Listeria* bacteriophage endolysin PlyP35 recognizes terminal GlcNAc residues in cell wall teichoic acid. Mol Microbiol 81:1419–1432. doi:10.1111/j.1365-2958.2011.07774.x

Fein JE, Rogers HJ (1976) Autolytic enzyme-deficient mutants of *Bacillus subtilis* 168. J Bacteriol 127:1427–1442

Fenton M, Keary R, McAuliffe O, Ross RP, O'Mahony J, Coffey A (2013) Bacteriophage-derived peptidase $CHAP_k$ eliminates and prevents staphylococcal biofilms. Int J Microbiol 2013:625341. doi:10.1155/2013/625341

Fernandes S, Proenca D, Cantante C, Silva FA, Leandro C, Lourenco S, Milheirico C, de Lencastre H, Cavaco-Silva P, Pimentel M, Sao-Jose C (2012) Novel chimerical endolysins with broad antimicrobial activity against methicillin-resistant *Staphylococcus aureus*. Microb Drug Resist 18:333–343. doi:10.1089/mdr.2012.0025

Finn RD, Bateman A, Clements J, Coggill P, Eberhardt RY, Eddy SR, Heger A, Hetherington K, Holm L, Mistry J, Sonnhammer EL, Tate J, Punta M (2014) Pfam: the protein families database. Nucleic Acids Res 42:D222–D230. doi:10.1093/nar/gkt1223

Fischetti VA (2008) Bacteriophage lysins as effective antibacterials. Curr Opin Microbiol 11:393–400. doi:10.1016/j.mib.2008.09.012

Fox LK, Zadoks RN, Gaskins CT (2005) Biofilm production by *Staphylococcus aureus* associated with intramammary infection. Vet Microbiol 107:295–299. doi:10.1016/j.vetmic.2005.02.005

Gaeng S, Scherer S, Neve H, Loessner MJ (2000) Gene cloning and expression and secretion of *Listeria monocytogenes* bacteriophage-lytic enzymes in *Lactococcus lactis*. Appl Environ Microbiol 66: 2951–2958. doi:10.1128/aem.66.7.2951-2958.2000

Grundling A, Schneewind O (2006) Cross-linked peptidoglycan mediates lysostaphin binding to the cell wall envelope of *Staphylococcus aureus*. J Bacteriol 188:2463–2472. doi:10.1128/JB.188.7.2463-2472.2006

Gu J, Lu R, Liu X, Han W, Lei L, Gao Y, Zhao H, Li Y, Diao Y (2011a) LysGH15B, the SH3b domain of staphylococcal phage endolysin LysGH15, retains high affinity to staphylococci. Curr Microbiol 63: 538–542. doi:10.1007/s00284-011-0018-y

Gu J, Xu W, Lei L, Huang J, Feng X, Sun C, Du C, Zuo J, Li Y, Du T, Li L, Han W (2011b) LysGH15, a novel bacteriophage lysin, protects a murine bacteremia model efficiently against lethal methicillin-resistant *Staphylococcus aureus* infection. J Clin Microbiol 49: 111–117. doi:10.1128/JCM.01144-10

Hadzija O (1974) A simple method for the quantitative determination of muramic acid. Anal Biochem 60:512–517. doi:10.1016/0003-2697(74)90261-9

Hazenberg MP, de Visser H (1992) Assay for *N*-acetylmuramyl-L-alanine amidase in serum by determination of muramic acid released from the peptidoglycan of *Brevibacterium divaricatum*. Eur J Clin Chem Clin Biochem 30:141–144

Hendrickx AP, van Schaik W, Willems RJ (2013) The cell wall architecture of *Enterococcus faecium*: from resistance to pathogenesis. Future Microbiol 8:993–1010. doi:10.2217/Fmb.13.66

Hovelius B, Mardh PA (1984) *Staphylococcus saprophyticus* as a common cause of urinary-tract infections. Rev Infect Dis 6:328–337. doi:10.1093/clinids/6.3.328

Jin JW, Zhang L, Zha XL, Li HL, Qu D (2005) Effect of glucose on biofilm and the gene *ica* expression in *Staphylococcus epidermidis* with different biofilm-forming capability. Acta Microbiol Sin 45: 431–436

Jones P, Binns D, Chang HY, Fraser M, Li W, McAnulla C, McWilliam H, Maslen J, Mitchell A, Nuka G, Pesseat S, Quinn AF, Sangrador-Vegas A, Scheremetjew M, Yong SY, Lopez R, Hunter S (2014) InterProScan 5: genome-scale protein function classification. Bioinformatics 30:1236–1240. doi:10.1093/bioinformatics/btu031

Kamisango K, Saiki I, Tanio Y, Okumura H, Araki Y, Sekikawa I, Azuma I, Yamamura Y (1982) Structures and biological-activities of peptidoglycans of *Listeria monocytogenes* and *Propionibacterium acnes*. J Biochem 92:23–33

Kumar S, Nei M, Dudley J, Tamura K (2008) MEGA: a biologist-centric software for evolutionary analysis of DNA and protein sequences. Brief Bioinform 9:299–306. doi:10.1093/bib/bbn017

Kuroda A, Sekiguchi J (1990) Cloning, sequencing and genetic mapping of a *Bacillus subtilis* cell wall hydrolase gene. J Gen Microbiol 136: 2209–2216. doi:10.1099/00221287-136-11-2209

Larkin MA, Blackshields G, Brown NP, Chenna R, McGettigan PA, McWilliam H, Valentin F, Wallace IM, Wilm A, Lopez R, Thompson JD, Gibson TJ, Higgins DG (2007) Clustal W and Clustal X version 2.0. Bioinformatics 23:2947–2948. doi:10.1093/bioinformatics/btm404

Leive L (1968) Studies on the permeability change produced in coliform bacteria by ethylenediaminetetraacetate. J Biol Chem 243:2373–2380

Loeffler JM, Nelson D, Fischetti VA (2001) Rapid killing of *Streptococcus pneumoniae* with a bacteriophage cell wall hydrolase. Science 294:2170–2172. doi:10.1126/science.1066869

Loessner MJ (2005) Bacteriophage endolysins-current state of research and applications. Curr Opin Microbiol 8:480–487. doi:10.1016/j.mib.2005.06.002

Loessner MJ, Kramer K, Ebel F, Scherer S (2002) C-terminal domains of *Listeria monocytogenes* bacteriophage murein hydrolases determine specific recognition and high-affinity binding to bacterial cell wall carbohydrates. Mol Microbiol 44:335–349. doi:10.1046/j.1365-2958.2002.02889.x

Melchior MB, Vaarkamp H, Fink-Gremmels J (2006) Biofilms: a role in recurrent mastitis infections? Vet J 171:398–407. doi:10.1016/j.tvjl.2005.01.006

Moreira JMR, Gomes LC, Araujo JDP, Miranda JM, Simoes M, Melo LF, Mergulhao FJ (2013) The effect of glucose concentration and shaking conditions on *Escherichia coli* biofilm formation in microtiter plates. Chem Eng Sci 94:192–199. doi:10.1016/j.ces.2013.02.045

Obeso JM, Martinez B, Rodriguez A, Garcia P (2008) Lytic activity of the recombinant staphylococcal bacteriophage phiH5 endolysin active against *Staphylococcus aureus* in milk. Int J Food Microbiol 128: 212–218. doi:10.1016/j.ijfoodmicro.2008.08.010

Oliveira H, Azeredo J, Lavigne R, Kluskens LD (2012) Bacteriophage endolysins as a response to emerging foodborne pathogens. Trends Food Sci Tech 28:103–115. doi:10.1016/j.tifs.2012.06.016

Oliveira H, Melo LD, Santos SB, Nobrega FL, Ferreira EC, Cerca N, Azeredo J, Kluskens LD (2013) Molecular aspects and comparative genomics of bacteriophage endolysins. J Virol 87:4558–4570. doi:10.1128/JVI.03277-12

Park KH, Kurokawa K, Zheng L, Jung DJ, Tateishi K, Jin JO, Ha NC, Kang HJ, Matsushita M, Kwak JY, Takahashi K, Lee BL (2010) Human serum mannose-binding lectin senses wall teichoic acid Glycopolymer of *Staphylococcus aureus,* which is restricted in infancy. J Biol Chem 285:27167–27175. doi:10.1074/jbc.M110.141309

Park J, Yun J, Lim JA, Kang DH, Ryu S (2012) Characterization of an endolysin, LysBPS13, from a *Bacillus cereus* bacteriophage. FEMS Microbiol Lett 332:76–83. doi:10.1111/j.1574-6968.2012.02578.x

Regulski K, Courtin P, Kulakauskas S, Chapot-Chartier MP (2013) A novel type of peptidoglycan-binding domain highly specific for amidated D-asp cross-bridge, identified in *Lactobacillus casei* bacteriophage endolysins. J Biol Chem 288:20416–20426. doi:10.1074/jbc.M112.446344

Salazar JK, Wu ZC, Yang WX, Freitag NE, Tortorello ML, Wang H, Zhang W (2013) Roles of a novel Crp/Fnr family transcription factor Lmo0753 in soil survival, biofilm production and surface attachment to fresh produce of *Listeria monocytogenes*. PLoS One 8: e75736. doi:10.1371/journal.pone.0075736

Schleifer KH, Kandler O (1972) Peptidoglycan types of bacterial cell walls and their taxonomic implications. Bacteriol Rev 36:407–477

Schmelcher M, Shen Y, Nelson DC, Eugster MR, Eichenseher F, Hanke DC, Loessner MJ, Dong S, Pritchard DG, Lee JC, Becker SC, Foster-Frey J, Donovan DM (2015) Evolutionarily distinct bacteriophage endolysins featuring conserved peptidoglycan cleavage sites protect mice from MRSA infection. J Antimicrob Chemoth 70: 1453–1465. doi:10.1093/jac/dku552

Shen Y, Koller T, Kreikemeyer B, Nelson DC (2013) Rapid degradation of *Streptococcus pyogenes* biofilms by PlyC, a bacteriophage-encoded endolysin. J Antimicrob Chemother 68:1818–1824. doi:10.1093/jac/dkt104

Simoes LC, Simoes M, Vieira MJ (2007) Biofilm interactions between distinct bacterial genera isolated from drinking water. Appl Environ Microbiol 73:6192–6200. doi:10.1128/Aem.00837-07

Son JS, Lee SJ, Jun SY, Yoon SJ, Kang SH, Paik HR, Kang JO, Choi YJ (2010) Antibacterial and biofilm removal activity of a podoviridae *Staphylococcus aureus* bacteriophage SAP-2 and a derived recombinant cell-wall-degrading enzyme. Appl Microbiol Biotechnol 86: 1439–1449. doi:10.1007/s00253-009-2386-9

Son B, Yun J, Lim JA, Shin H, Heu S, Ryu S (2012) Characterization of LysB4, an endolysin from the *Bacillus cereus*-infecting bacteriophage B4. BMC Microb 12:33. doi:10.1186/1471-2180-12-33

Szweda P, Schielmann M, Kotlowski R, Gorczyca G, Zalewska M, Milewski S (2012) Peptidoglycan hydrolases-potential weapons against *Staphylococcus aureus*. Appl Microbiol Biotechnol 96: 1157–1174. doi:10.1007/s00253-012-4484-3

Theodoros Kelesidis ST (2010) *Staphylococcus intermedius* is not only a zoonotic pathogen, but may also cause skin abscesses in humans after exposure to saliva. Int J Infect Dis 14:e838–e841. doi:10.1016/j.ijid.2010.02.2249

Voineagu L, Braga V, Botnarciuc M, Barbu A, Tataru M (2012) Emergence of *Staphylococcus hominis* strains in general infections. ARS Medica Tomitana 18:80–82. doi:10.2478/v10307-012-0016-8

Won YS, Kwon HJ, Oh GT, Kim BH, Lee CH, Park YH, Hyun BH, Choi YK (2002) Identification of *Staphylococcus xylosus* isolated from C57BL/6 J-*Nos2*^{tm1Lau} mice with dermatitis. Microbiol Immunol 46:629–632

Wu JA, Kusuma C, Mond JJ, Kokai-Kun JF (2003) Lysostaphin disrupts *Staphylococcus aureus* and *Staphylococcus epidermidis* biofilms on artificial surfaces. Antimicrob Agents Chemother 47:3407–3414. doi:10.1128/aac.47.11.3407-3414.2003

Yang H, Zhang Y, Huang Y, Yu J, Wei H (2014a) Degradation of methicillin-resistant *Staphylococcus aureus* biofilms using a chimeric lysin. Biofouling 30:667–674. doi:10.1080/08927014.2014.905927

Yang H, Zhang Y, Yu J, Huang Y, Zhang XE, Wei H (2014b) Novel chimeric lysin with high-level antimicrobial activity against methicillin-resistant *Staphylococcus aureus in vitro* and *in vivo*. Antimicrob Agents Chemother 58:536–542. doi:10.1128/AAC.01793-13